Performance Analysis of a Multiport Encoder/Decoder in OCDMA Scenario

Gianluca Manzacca, *Student Member, IEEE*, Anna Maria Vegni, Xu Wang, *Senior Member, IEEE*, Naoya Wada, *Member, IEEE*, Gabriella Cincotti, *Senior Member, IEEE*, and Ken-ichi Kitayama, *Fellow, IEEE*

***Abstract*—We investigate the use of a single multiport encoder/decoder in an optical code-division multiple access network scenario. We present a comparison between the performance of two sets of phase-shifted keying codes, and evaluate the bit error rate and the spreading effect due to the asynchronous access. We also investigate the performance degradation due to the presence of both multiple access interference and beat noises.**

***Index Terms*—Monitoring, Codecs, coding, communication system routing, decoding, optical correlators.**

I. Introduction

The growing demand for communication services from residential costumers is one of the main spurs for the introduction of optical code-division multiple access (OCDMA) technique into access networks. Since the last decade, many different architectures have been proposed to implement efficient large-band last-mile networks, but the most cost-effective solutions, in terms of upgrade ability and flexibility, are passive optical networks (PONs) [1]. Time-division multiplexing (TDM) [2] and wavelength-division multiplexing (WDM) [3] approaches have been largely experimented: TDM-based PONs based on asynchronous transfer module (ATM) protocol or Ethernet protocol allow the sharing of transmission from 155 Mb/s up to 1 Gb/s among 8–32 users [4]. However, TDM-based PONs cannot adapt the bit rate in the uplink transmission according to different requests from different users. WDM-based PONs enhance the uplink capacity, assigning a single wavelength between the optical line terminal (OLT) and the optical network unit (ONU) [3].

OCDMA technique introduces a new dimension in multiple access schemes over standard time and frequency domains, and allows asynchronous transmission, provides more flexible bandwidth usage, in terms of granularity, that can also be provisioned, and improves the network confidentiality. Code-based access schemes are classified depending on the coherence of the sources, and the coding and detection methods.

A coherent OCDMA network requires highly coherent sources, such as mode-locked laser diodes (MLLDs), whereas a low-cost LED can be used in incoherent systems. Many different techniques have been proposed in literature to generate optical codes, both in the time and frequency domains. In the first case, the input laser pulse is split into a set of chips that are intensity modulated in the case of incoherent optical orthogonal codes (OOCs) [5], or phase modulated using superstructured fiber Bragg gratings (SSFBGs) to generate phase-shifted keying (PSK) codes [6], [7]. Using the frequency-domain coding techniques, the spectral content of a broadband input laser pulse is modulated using either bulk-optics elements, such as gratings, lenses, and phase masks, or planar arrayed waveguide gratings (AWGs) and phase/amplitude modulators. The encoding process is based on the Fourier transform, and it does not require high-frequency optical modulators that are used in time-domain encoding systems [8], [9]. Other coding schemes, based on incoherent sources, have been proposed using optical fast frequency hopping (OFFH) techniques, where each chip has a different wavelength; the orthogonality condition depends on the code weights and the frequency slots [10].

Fig. 1. describes several conventional encoding/decoding schemes. Fig. 1(a) shows the architecture of a passive OOC generator, which consists of a splitter, a bank of delay lines, an electronic circuit for the code selection, and a combiner. The decoding process is performed in the electric domain and a suitable clock recovery circuit is required [11]. Fig. 1(b) shows a spectral encoding technique, where a phase mask is used to encode a broadband pulse; in this case, the decoding process is reciprocal to the encoding scheme. A planar lightwave circuit (PLC) device that is able to generate PSK codes is described in Fig. 1(c) and consists of tunable taps and phase shifters; this architecture is characterized by a flexible tunability, but it presents some drawbacks, compared to SSFBG, such as polarization dependence and the impossibility to realize long code sequences due to fabrication constraints [12]. Finally, Fig. 1(d) shows a scheme for the frequency hopping technique, where the broadband pulse is encoded using a number of chips at different subbands.

A proper choice of the detection method can enhance the system performances: for instance, in coherent OCDMA schemes, it is possible to use time gating if all the users are synchronous; in that case, the gain equates the spreading factor. Optical thresholding, which can be based on supercontinuum generation in a nonlinear fiber [13], reduces the out-of-band noise because the interfering signals are too weak to produce a nonlinear effect.

Ten truly asynchronous users have been OCDMA multiplexed in [14], using PSK Gold codes, optical thresholding, and time gating to suppress the multiple access interference (MAI) noise.

Manuscript received November 28, 2006; revised March 12, 2007.

G. Manzacca, A. M. Vegni, and G. Cincotti are with the University of Roma Tre, Rome I-00146, Italy (e-mail: manzacca@uniroma3.it; avegni@uniroma3.it; cincotti@uniroma3.it).

X. Wang and N. Wada are with the National Institute of Information and Communication Technology (NICT), Tokyo 184-879, Japan (e-mail: xwang@nict.go.jp; wada@nict.go.jp).

K.-i. Kitayama is with the Department of Electrical, Electronics and Information Systems, Osaka University, Osaka 565-0871, Japan (e-mail: kitayama@comm.eng.osaka-u.ac.jp).

Digital Object Identifier 10.1109/JSTQE.2007.897607

1077-260X/$25.00 © 2007 IEEE

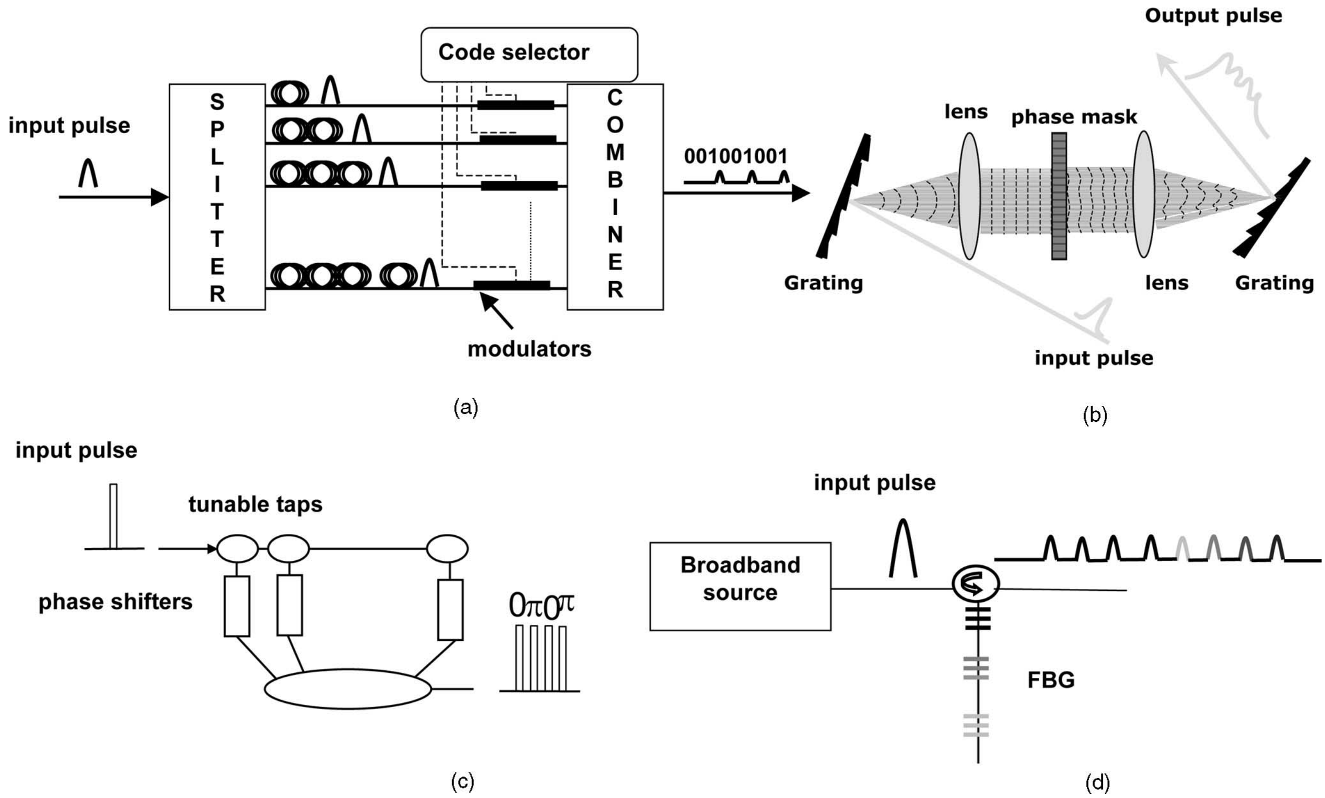

Fig. 1. Four different optical encoding schemes. (a) Planar architecture to generate OOCs. (b) Bulk optics scheme that generates frequency spread-spectrum codes. (c) Planar tunable device to generate PSK codes. (d) FBG-based scheme to build OFFH codes.

The PSK codes are generated using an SSFBG, which makes 511 copies of the input pulse, each of them with a different phase information. We described in [15]–[17] a new planar multiport encoder/decoder (E/D), in an AWG configuration, that is able to generate and process simultaneously a set of different coherent codes. A broadband input pulse is filtered by the transfer function of the device, and N different PSK codes are generated, where N is the number of the output ports. The decoding process is performed using the same device: forwarding the encoded pulse into one of the decoder input ports, the autocorrelation signal is measured at one output, whereas at the other outputs, we measure the cross-correlation signals.

The encoding process is a time-based technique: the input slab coupler makes N copies of the input laser pulse, which travel the grating arms with different delays. The chips are combined by the output slab coupler to generate N codes at the device output ports [17]. On the other hand, the orthogonal property of the codes can be explained by using a frequency-domain analysis: the cross-correlation function between two different codes vanishes because its Fourier transform is the product of two nonoverlapping frequency spectra. From this analysis, it is also evident that the codes generated at adjacent ports are "less orthogonal," i.e., the corresponding power contrast ratio (PCR), i.e., the ratio between the autocorrelation peak (ACP) and the maximum cross-correlation peak (CCP) is the lowest.

Some previous experiments of pulse train generation have been reported by Leaird *et al.* in [18] and [19], which are similar to the proposed encoding scheme: the main difference is that the AWG-based E/D simultaneously generates a set of codes that are composed of chips with different phases. The Rowland circle configurations at the input/output slabs have been selected to generate the chip phases.

The E/D generates a set of OOCs that allow N users to access the network simultaneously in an asynchronous way. For this reason, we can classify the proposed scheme as an OCDMA transmission; in contrast to standard spread spectrum techniques, different codes correspond to different frequency subbands, and therefore, the users do not share the same bandwidth, even though they transmit at the same wavelength. However, this OCDMA scheme can be used in conjunction with standard WDM transmission, and an hybrid experiment has been reported in [20] for ten OCDMA users and three wavelengths.

In the present paper, we evaluate the performance of PSK codes, generated by a single multiport E/D, considering synchronous and asynchronous transmission, and both MAI and beat noises. The rest of the paper is organized as follows. In Section II, we compare two different sets of PSK codes, and investigate the performance of Gold codes of different lengths generated by an SSFBG and the codes generated by an AWG-based encoder in a synchronous transmission, considering only the MAI noise. These two PSK code families are generated by using a time-spreading encoding technique, by making copies of a single broadband pulse. Gold codes present good correlation properties that are comparable to those of the PSK codes generated by the multiport E/D, but the code sequences are much longer. The ACP from a Gold code sequence is very sharp, and it is possible to reduce the influence of the beat noise by using time gating and optical thresholding [14]. On the other hand, PSK codes generated by the multiport E/D present a very large autocorrelation signal, and therefore, optical thresholding is not possible for this class of codes. We consider a synchronous transmission to investigate the worst case condition, and to evidence the code performance, we analyze only MAI noise.The influence of the beat noise on the performance of Gold codes has been investigated in [25], and similar results are obtained for the proposed PSK codes in Section IV. The asynchronous OCDMA systems that use AWG-based devices are described in Section III; in Section IV, we present an accurate model for the beat noise that is dominant in an OCDMA transmission. Comparing these results with those of [25], we can evidence that the AWG-based E/D allows us to multiplex up to eight users without reaching the floor performance, whereas the maximum number of users using Gold code is 3. Therefore, the proposed multiport E/D can be a cost-effective solution for a broadband access network, since no external devices are required to suppress beat noise.

Finally, we analyze the performance degradation due to polarization scrambling and the asynchronous transmission of interfering channels in terms of noise variance, and conclusions are given in the last section.

II. Comparison of Two PSK Code Families

PSK codes generated by an SSFBG have been proven to be very effective in OCDMA transmissions [14], and a comparison of the PCR parameters corresponding to the codes generated by the AWG-based device and the SSFBG has been presented in [21]. We observed that the ratio between the ACPs and CCPs for Gold codes is lower than 1.5 dB, whereas it is larger than 5 dB for codes generated by the AWG-based E/D.

In this section, we compare the performance of these two PSK code families, evaluating the bit error rate (BER) and considering synchronous transmission and only the MAI noise. In this way, we analyze the worst case scenario when all users interfere coherently.

BER for PSK codes has been evaluated in [22] as

$$\begin{aligned}\mathrm{BER}(n) &= 1-\frac{1}{4}\prod_{i=n+1}^{N} \\ &\times\left\{1+\operatorname{erf}\left[\sqrt{\frac{\mathrm{SNR}}{8}}\left(1+\frac{\mathrm{CCP}_{\max}^2-2(\mathrm{CCP}_i^n)^2}{(\mathrm{ACP}_i^n)^2}\right)\right]\right\} \\ &\times\prod_{i=1}^{n}\operatorname{erfc}\left[\sqrt{\frac{\mathrm{SNR}}{8}}\left(\frac{\mathrm{CCP}_{\max}^2-(\mathrm{ACP}_i^n)^2}{(\mathrm{ACP}_i^n)^2}\right)\right] \end{aligned} \quad (1)$$

where n is the number of simultaneously interfering users that transmit a logic "1", $\mathrm{SNR}=\mathrm{ACP}^4/\sigma^2$, and σ^2 is the variance of noise with Gaussian statistic and zero mean. We suppose that the noise statistic at the receiver is the same for all the codes, and the crosstalk is described as an in-band noise. The performance

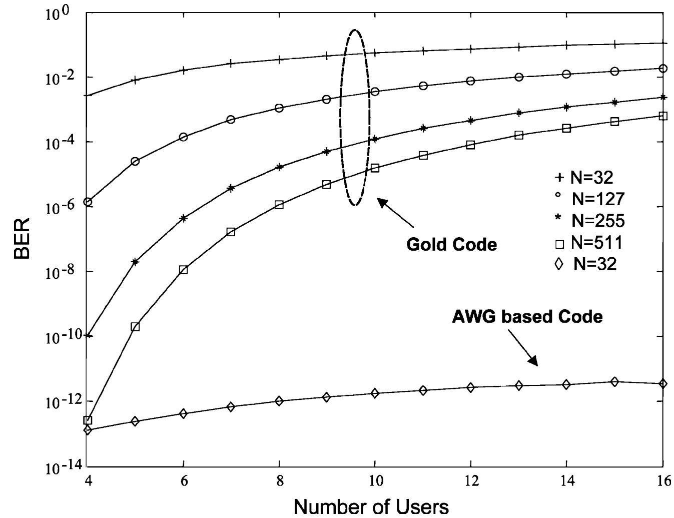

Fig. 2. BER versus the number of users: comparison between codes generated by the multiport device (rhombus) and Gold codes with different lengths.

degradation in a multiuser environment is due to the coherent sum of the signals detected at the receiver. In the case of synchronous transmission, the auto- and cross-correlation signals interfere with each other, and ACP_i^n detected at port i when n users are simultaneously transmitting a "1" is larger than the value corresponding to a single user transmission ACP; the same effect can be observed for CCP_i^n.

To reduce the MAI noise, we use not only the adjacent ports but also the ACP and CCP, which are, respectively, given by

$$\mathrm{ACP}_{2i}^n = \mathrm{ACP}+\sum_{j=1}^{n}\mathrm{CCP}_{2j}, \qquad i=1,2,\ldots,N/2 \quad (2)$$

$$\mathrm{CCP}_{2i}^n = \sum_{j=1}^{n}\mathrm{CCP}_{2j}, \qquad i=1,2,\ldots,N/2. \quad (3)$$

In a synchronous access network, the number of active users should be known *a priori*, or estimated in real time in order to dynamically set the threshold level; we evaluate the network performances in the worst case condition, when the threshold level is fixed to $I_{\mathrm{th}}=\left(\mathrm{ACP}_{\min}^2+\mathrm{CCP}_{\max}^2\right)/2$, and $\mathrm{CCP}_{\max}$ and $\mathrm{ACP}_{\min}$ have been evaluated when all the even ports of the device have been used.

The performances of Gold codes of length L have been analyzed in [4] as

$$\mathrm{BER}(L,n)=\frac{1}{2}\operatorname{erfc}\left(\frac{\mathrm{Th}}{\sqrt{2}}\sqrt{\mathrm{SNR}(L,n)}\right) \quad (4)$$

where Th is the normalized threshold, which is set to 1 in the most favorable case, and

$$\mathrm{SNR}(L,n)=\frac{1}{\sigma^2(L)(n-1)}. \quad (5)$$

BER is plotted in Fig. 2 as a function of the number of active users for different Gold codes of lengths 31, 127, 255, and 511 chips, and for the PSK codes generated by the AWG-based device with 32 ports. The threshold value for Gold codes has

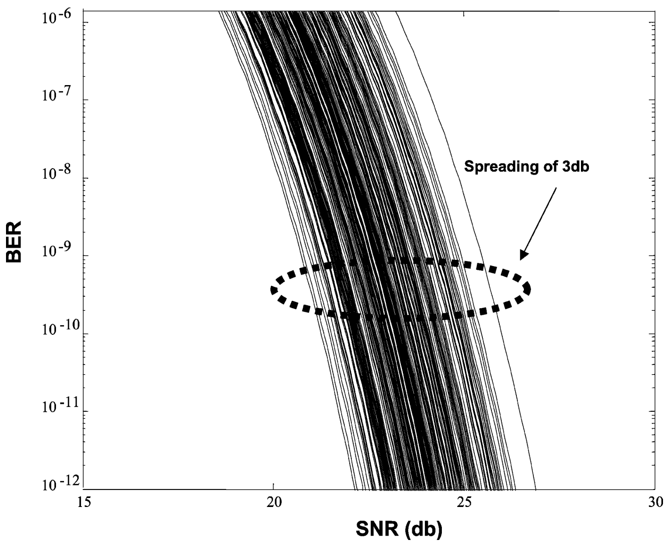

Fig. 3. BER versus the SNR in an OCDMA asynchronous transmission with 32 interfering users.

been set to 1, their variances have been calculated as described in [23], and we assumed that the SNR is equal to the value corresponding to only one interfering user using a Gold code of 511 chips. From an inspection of this figure, it is evident that the PSK codes from the AWG-based device have superior performance, especially for a large number of simultaneous users.

III. Asynchronous OCDMA

In an asynchronous OCDMA scenario, two main random parameters have to be taken into account: the number of users transmitting simultaneously and their reciprocal delays [24]. In an asynchronous OCDMA, the BER can be evaluated as [17]

$$\begin{aligned}\mathrm{BER}(n) &= 1-\frac{1}{2}\\ &\times\left\{\frac{1}{2}+\frac{1}{2}\mathrm{erf}\left[\sqrt{\frac{\mathrm{SNR}}{8}}\left(1+\frac{(\mathrm{CCP}_{\max})^2}{(\mathrm{ACP}_i^n)^2}-2\frac{(\mathrm{CCP}_i^n)^2}{(\mathrm{ACP}_i^n)^2}\right)\right]\right\}\\ &-\frac{1}{2}\left\{\frac{1}{2}\mathrm{erfc}\left[\sqrt{\frac{\mathrm{SNR}}{8}}\left(\frac{(\mathrm{CCP}_{\max})^2}{(\mathrm{ACP}_i^n)^2}+1-2\frac{(\mathrm{ACP}_i^n)^2}{(\mathrm{ACP}_i^n)^2}\right)\right]\right\}.\end{aligned} \tag{6}$$

We assume that the number of simultaneously transmitting users n is a random variable that can be described by a Bernoulli distribution, whereas their relative random delays have a uniform distribution around the synchronous case. The BER of a transmission system with 32 asynchronous users is plotted in Fig. 3. We observe a spreading of the performance due to the random sum of the phases of the fields of each code of 3 dB around the synchronous case.

IV. Beat Noise Model

In the previous sections, we compared synchronous and asynchronous OCDMA systems, considering only the MAI noise,

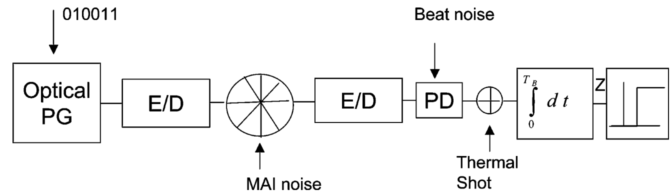

Fig. 4. Transmissionscheme of an OCDMA network.

but a more accurate model also takes into account the beat noise generated at the photodetector (see Fig. 4). A closed form of the total integrated power of the autocorrelation signal can be evaluated as [17]

$$\begin{aligned}A_{\mathrm{ac}} &= \sum_{j=0}^{N-1}\int_0^{T_b}\left|(j+1)\exp\left[-\frac{(t-j\,\Delta\tau)^2}{2\sigma}\right]\right|^2 dt\\ &+\sum_{j=N}^{2N-2}\int_0^{T_b}\left|(2N-j-1)\exp\left[-\frac{(t-j\,\Delta\tau)^2}{2\sigma}\right]\right|^2 dt\end{aligned} \tag{7}$$

and if we suppose $\sigma \ll \Delta\tau$, A_{ac} can be simplified as

$$A_{\mathrm{ac}} = \frac{N(2N^2+1)}{3}A_G \tag{8}$$

where A_G is the integrated intensity of an input Gaussian pulse. A similar expression can be obtained for the integrated power of the cross-correlation signal

$$\begin{aligned}A_{\mathrm{cc}}(k-k') &= \sum_{j=0}^{2N-2}\int_0^{T_b}\left|\frac{\sin\left[\pi(j+1)(k-k')/N\right]}{\sin\left[\pi(k-k')/N\right]}\right.\\ &\quad\left.\times\exp\left[-\frac{(t-j\,\Delta\tau)^2}{2\sigma^2}\right]\right|^2 dt\\ &\qquad k',k=0,1,\ldots,N-1\end{aligned} \tag{9}$$

and after simple algebra, we obtain

$$\begin{aligned}A_{\mathrm{cc}}\,(k-k') &= \csc^2\left[\frac{\pi\,(k-k')}{N}\right]\left\{N-\frac{1}{4}\,\sin\left[(4N-1)\,\pi(k-k')\right]\right.\\ &\quad\left.\times\frac{1}{4}\,\csc\left[\pi\,(k-k')\right]\right\}A_G.\end{aligned} \tag{10}$$

Considering the scheme of Fig. 4, the decision metrics Z can be expressed as

$$\begin{aligned}Z &= \Re\int_0^{T_b} E_1^2\,(t)\;dt\\ &+\Re\sum_{i=2}^{N}\int_0^{T_b} 2E_1\,(t)\,E_i\,(t)\,\cos\left[\phi_1\,(t)-\phi_i\,(t)\right]\,dt\\ &+\Re\sum_{i,j=2(i>j)}^{N}\int_0^{T_b} 2E_i\,(t)\,E_j\,(t)\,\cos\left[\phi_i\,(t)-\phi_j\,(t)\right]\,dt\\ &+\Re\sum_{i=2}^{N}\int_0^{T_b} E_i^2(t)\,dt+n(t)\end{aligned} \tag{11}$$

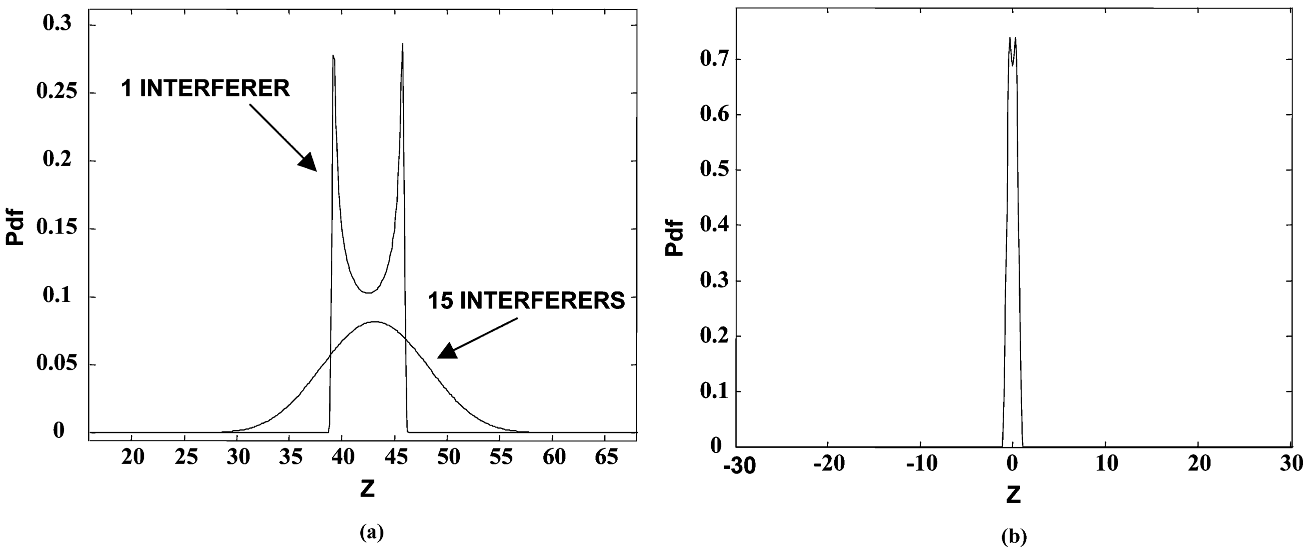

Fig. 5. (a) Probability density function of the photocurrent detected at port 1 with 15 other interfering channels. The first beat noise and the thermal noise have been taken into account. (b) Probability density function of the second beat noise term.

where E_1 is the field amplitude of the signal from user 1, with phase ϕ_1, $E_i \exp(\phi_i)$'s are the interfering signals from the other users, and $\Re$ is the responsivity of the photodetector. In this expression, the first term is the desired signal from user 1, the second and the third terms are the first and the second beat noises, the fourth one is the MAI noise, and the last one represents a Gaussian random process with variance $\sigma^2 = \sigma_{\rm th}^2 + \sigma_{\rm sh}^2$, due to thermal and shot noises. For our codes, we need to take into account the beat noise as we generate codes through a source where $\tau_c \geq T_c$ with τ_c the coherence time of the source and T_c the chip duration: as all chips of an encoded bit are generated from a passive device, the coherence of the phase between two different interfering channel is kept for all the integration time T_b, and so, we cannot neglect the beat terms in (11).

The probability density function (pdf) of the photocurrent detected at port 1 is plotted in Fig. 5(a), considering 15 interfering channels and only the contributions of the first beat noise term and the thermal noise. The pdf of the second beat term is represented in Fig. 5(b), and we observe that it has a delta-like shape and does not affect the detection; therefore, in our numerical evaluations, we consider only the first beat noise, assuming a Gaussian statistic, which becomes more accurate for a large number of users, with variance

$$\sigma_{\rm beat}^2 = 2\Re^2 \sum_{i=2}^{N} \int_0^{T_b} E_1^2(t) E_i^2(t)\, dt. \tag{12}$$

The variance of the whole noise is $\sigma_{\rm tot}^2 = \sigma_{\rm beat}^2 + \sigma_{\rm sh}^2 + \sigma_{\rm th}^2$, and the pdf for logic "1" and "0" are, respectively, given by

$$P_x^{(1)}(x) = \frac{1}{\sqrt{2\pi\sigma_{\rm tot}^2}} \exp\left[\frac{\left(x - A_{\rm ac} - \sum_{i=2}^{N} A_{\rm cc}(i)\right)^2}{2\sigma_{\rm tot}^2}\right] \tag{13}$$

$$P_x^{(0)}(x) = \frac{1}{\sqrt{2\pi\sigma_{\rm th}^2}} \exp\left[\frac{\left(x - \sum_{i=2}^{N} A_{\rm cc}(i)\right)^2}{2\sigma_{\rm th}^2}\right]. \tag{14}$$

The total error probability can be expressed as

$$P_e = \frac{1}{4}\left(1 + \mathrm{erf}\left[\frac{\Re\left(A_{\rm ac} - \mathrm{Th}\, A_{\rm ac} - \mathrm{Th} \sum_{i=1}^{N} A_{\rm cc}(i)\right)}{\mathrm{Th}\sqrt{2\sigma_{\rm tot}^2}}\right] + \mathrm{erfc}\left[\frac{\Re\left(A_{\rm ac} - \mathrm{Th}\sum_{i=1}^{N} A_{\rm cc}(i)\right)}{\mathrm{Th}\sqrt{2\sigma_{\rm th}^2}}\right]\right) \tag{15}$$

where $\sigma_{\rm th}^2 = B_r N_{\rm th} \gg \sigma_{\rm sh}^2$, with B_r the receiver bandwidth, and $N_{\rm th}$ is the thermal noise spectral density, with a typical value of 1 pA^2/Hz [25].

The BER of a synchronous access of eight users as a function of the detected power is plotted in Fig. 6; the threshold used is $\mathrm{Th} = 2$. From an inspection of this figure, we observe the dominance of the first beat noise term, and that the Gaussian approximation is an overestimation of the real noise statistic.

In an actual OCDMA network, each user transmits with a different polarization, and their statistic independence improves the system's performances, since the contribution of interfering channels to the power of the beat noise has the following expression:

$$\sigma_{\rm beat}^2 = \frac{\Re^2}{\pi} \sum_{i=2}^{N} \int_0^{2\pi} \int_0^{T_b} E_1^2(t) E_i^2(t) \cos^2\theta_i \, dt\, d\theta_i \tag{16}$$

where θ_i is a random variable with a uniform distribution between 0 and 2π; therefore, the variance is reduced by 0.5. If we consider a random delay between channel 1 and the interfering

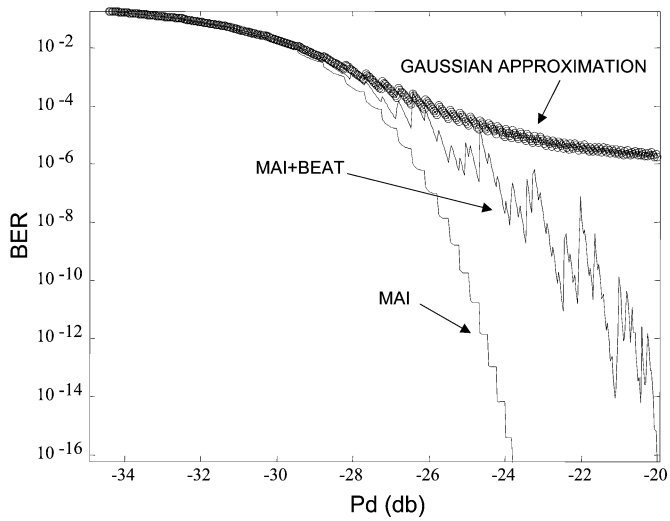

Fig. 6. BER of a synchronous transmission of eight users: the dotted line refers to the case where only MAI and thermal noise have been taken into account; the continuous line represents the performances when both MAI and the real statistic of beat noise have been considered; the circled line refers to the case where we considered both MAI and a Gaussian approximation of the beat noise.

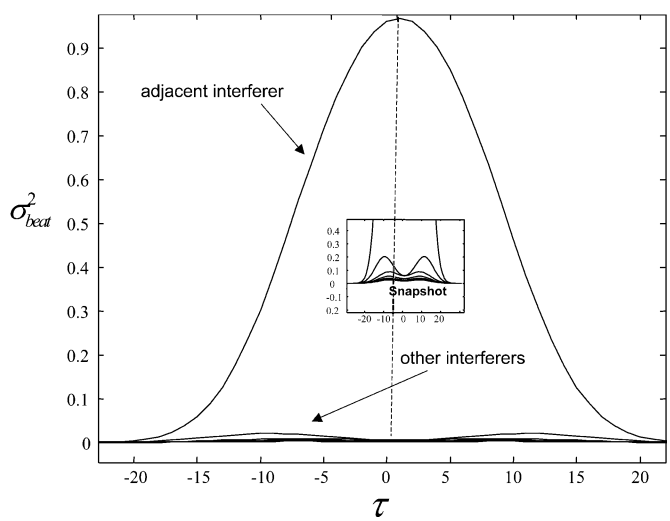

Fig. 7. Normalizedvariance of first beat noise versus the time delay (τ): all the contribution from the interfering channels are plotted separately. The variable τ has been normalized to the input pulse width.

channels, we obtain

$$\sigma^2_{\mathrm{beat}} = \frac{\Re^2}{T_b}\sum_{i=2}^{N}\int_{-T_b}^{T_b}\int_{-T_b/2}^{T_b/2} E_1^2(t)E_i^2(t+\tau_i)\,dt\,d\tau_i \qquad (17)$$

which is plotted in Fig. 7.

V. Conclusion

In the present paper, we analyzed the performance of a multiport E/D: we compared the performance of optical Gold codes and PSK codes generated by a multiport E/D considering only the MAI noise, and showed that the PSK codes have better performance as the number of interferer users is large. We also presented a more accurate model of the transmission system that also takes into account the beat noise, and demonstrated that the first beat term due to the interferer channels on the desired signal is the most important source of noise: the degradation due to the beat noise is about 3 dB for a BER $= 10^{-9}$. The performances of the asynchronous scenario have been analyzed, considering both MAI and beat noises.

References

[1] P. Green, "Paving the last mile with glass," *IEEE Spectr.*, vol. 39, no. 12, pp. 13–14, Dec. 2002.

[2] A. Tan, "Super PON-A fiber to the home cable network for CATV and POTS/ISDN/VOD as economical as a coaxial cable network," *J. Lightw. Technol.*, vol. 15, no. 2, pp. 213–218, Feb. 1997.

[3] G. Maier, M. Martinelli, and A. Pattavina and Salvadori, "Design and cost performance of multistage WDM-PON access network," *J. Lightw. Technol.*, vol. 18, no. 2, pp. 125–143, Feb. 2000.

[4] K.-i. Kitayama, X. Wang, and N Wada, "OCDMA Ower WDM PON-solution path to gigabit-symmetric FTTH," *J. Lightw. Technol.*, vol. 24, no. 4, pp. 1654–1662, Apr. 2006.

[5] J. A. Salehi, "Emerging optical code-division multiple access communication systems," *IEEE Netw.*, vol. 3, no. 2, pp. 31–39, Mar. 1989.

[6] P. C. Teh, P. Petropoulos, M. Ibsen, and D. J. Richardson, "Phase encoding and decoding of short pulses at 10 Gb/s using superstructured fiber Bragg gratings," *IEEE Photon. Technol. Lett.*, vol. 13, no. 2, pp. 154–156, Feb. 2001.

[7] X. Wang, K. Matsushima, A. Nishiki, N. Wada, and K.-I. Kitayama, "High reflectivity superstructured FBG for coherent optical code generation and recognition," *OSA Opt. Exp.*, vol. 12, no. 12, pp. 5457–5468, Nov. 2004.

[8] A. Weiner, J. Heritage, and J. Salehi, "Encoding and decoding of femtosecond pulses," *Opt. Lett.*, vol. 13, pp. 300–302, 1988.

[9] J. Heritage, A. Weiner, and R. Thurston, "Picosecond pulse shaping by spectral phase and amplitude manipulation," *Opt. Lett.*, vol. 10, pp. 609–611, 1985.

[10] H. Fathallah, L. Rusch, and S. LaRochelle, "Passive optical fast frequency-hop CDMA communications system," *J. Lightw. Technol.*, vol. 17, no. 3, pp. 397–405, Mar. 1999.

[11] A. Keshvarzian and J. A. Salehi, "Multiple-shift code acquisition of optical orthogonal codes in optical CDMA systems," *IEEE Trans. Commun.*, vol. 53, no. 4, pp. 687–698, Apr. 2005.

[12] K.-i. Kitayama, N. Wada, and H. Sotobayashi, "Architectural considerations for photonic IP router based upon optical code correlation," *J. Lightw. Technol.*, vol. 18, no. 12, pp. 1834–1844, Dec. 2000.

[13] T. Okuno, M. Onishi, and M. Nishimura, "Generation of ultra-braod-band supercontinuum by dispersion-flattened and decreasing fiber," *IEEE Photon. Technol. Lett.*, vol. 10, no. 1, pp. 72–74, Jan. 1998.

[14] T. Hamanaka, X. Wang, N. Wada, A. Nishiki, and K.-i. Kitayama, "Ten-user truly asynchronous gigabit OCDMA transmission experiment with a 511-chip SSFBG en/decoder," *J. Ligthw. Technol.*, vol. 24, no. 1, pp. 95–102, Jan. 2006.

[15] G. Cincotti, "Full optical encoders/decoders for photonic IP routers," *J. Lightw. Technol.*, vol. 22, no. 2, pp. 337–342, Feb. 2004.

[16] G. Cincotti, "Design of optical full encoders/decoders for code-based photonic routers," *J. Lightw. Technol.*, vol. 22, no. 7, pp. 1642–1650, Jul. 2004.

[17] G. Cincotti, N. Wada, and K.-i. Kitayama, "Characterization of a full encoder/decoder in the AWG configuration for code-based photonic routers. Part I: Modelling and design," *J. Lightw. Technol.*, vol. 24, no. 1, pp. 103–112, Jan. 2006.

[18] D. E. Leaird, S. Shen, A. M. Weiner, A. Sugita, S. Kamei, M. Ishii, and K. Okamoto, "Generation of high-ripetition-rate WDM pulse trains from an arrayed-waveguide grating," *IEEE Photon. Technol. Lett.*, vol. 13, no. 3, pp. 221–223, Mar. 2001.

[19] D. E. Leaird, A. M. Weiner, S. Kamei, M. Ishii, A. Sugita, and K. Okamoto, "Generation of flat-topped 500-GHz pulse burst using loss engineered arrayed-waveguide gratings," *IEEE Photon. Technol. Lett.*, vol. 14, no. 6, pp. 816–818, Jun. 2002.

[20] R. X. Wang, N. Wada, T. Miyazaki, G. Cincotti, and K.-i. Kitayama, "Field trail of 3-WDM × 10-OCDMA × 10.71 Gbps, truly asynchronous, WDM/DPSK-OCDMA using hybrid E/D without FEC and optical threshold," (Postdeadline paper), presented at the Opt. Fiber Commun. Conf. (OFC), Anaheim, CA, 2006.

[21] X. Wang, N. Wada, G. Cincotti, T. Miyazaki, and K. Kitayama, "Demonstration of over 128-Gb/s-capacity (12-users $\times$ 10.71-Gb/s/user) asynchronous OCDMA using FEC and AWG-based multiport optical encoder/decoders," *IEEE Photon. Technol. Lett.*, vol. 18, no. 15, pp. 1603–1605, Aug. 2006.

[22] G. Manzacca, M. Svaluto Moreolo, and G. Cincotti, "Performance analysis of multi-dimensional codes generated/processed by a single planar device," *J. Lightw. Technol.*, 2007, to be published.

[23] M. B. Pursley, "Performance evaluation for phase-coded spread-spectrum multiple-access communication—Part I: System analysis," *IEEE Trans. Commun.*, vol. COM-25, no. 8, pp. 795–799, Aug. 1977.

[24] W. Kwong, P. A. Perrier, and P. R. Prucnal, "Performance comparison of asynchronous and synchronous code-division multiple-access techniques for fiber-optic local area network," *IEEE Trans. Commun.*, vol. 39, no. 11, pp. 1625–1634, Nov. 1991.

[25] X. Wang and K. Kitayama, "Analysis of the beat noise in coherent and incoherent yime-spreading OCDMA Network," *J. Lightw. Technol.*, vol. 22, no. 10, pp. 2226–2235, Oct. 2004.

Gianluca Manzacca (S'06) was born in Cernusco sul Naviglio, Italy, in March 1981. He received the Laurea (M.Sc.) degree (cum laude) in electronic engineering in March 2005 from the University of Roma Tre, Rome, Italy, where he is currently working toward the Ph.D. degree in telecommunication engineering.

His current research interests include optical communication, photonic crystal, and quantum optics.

Mr. Manzacca is a Student Member of the IEEE Laser and Electro-Optics Society (LEOS) and a member of the National Inter-University Consortium for Telecommunications (CNIT).

Anna Maria Vegni was born in Rome, Italy, on July 24, 1982. She received the first-level Laurea and second-level Laurea (Laurea Magistralis) degrees (cum laude) in electronics engineering in July 2004 and July 2006, respectively, from the University of Roma Tre, Rome, where she is currently working toward the Ph.D. degree in biomedical engineering, electromagnetic and telecommunications.

Her current research interests include quality-of-service (QoS) and optical networking, signal and image processing, security in telecommunication systems, and biometrics.

Xu Wang (S'91–M'98–SM'06) received the B.S. degree in physics from Zhejiang University, Hangzhou, China, in 1989, the M.S. degree in electronics engineering from the University of Electronics Science and Technology of China (UESTC), Chengdu, China, in 1992, and the Ph.D. degree in electronics engineering from the Chinese University of Hong Kong (CUHK), Hong Kong, in 2001.

From 1992 to 1997, he was a Lecturer at the National Key Laboratory of Fiber Optic Broad-Band Transmission and Communication Networks, UESTC. During 2001–2002, he was a Postdoctoral Research Fellow in the Department of Electronic Engineering, CUHK. From 2002 to 2004, he was a Telecommunications Advancement Organization (TAO) Research Fellow with the Department of Electronic and Information Systems, Osaka University, Osaka, Japan. Since April 2004, he has been a Researcher with the Ultra-Fast Photonic Network Group, Information and Network Systems Department, National Institute of Communication and Information Technology (NICT), Tokyo, Japan. He is also an adjunct Professor at a couple of universities in China. His current research interests include fiber optic communication networks, optical code-division multiplexing, optical packet switching, semiconductor laser, application of fiber gratings, and fiber optic signal processing. He has filed three patents and is the first author of more than 70 technical papers.

Dr. Wang was awarded the Telecommunications Advancement Research Fellowship by the TAO, Japan, in 2002 and 2003.

Naoya Wada (M'97) received the B.E., M.E., and Dr.Eng. degrees in electronics from Hokkaido University, Sapporo, Japan, in 1991, 1993, and 1996, respectively.

In 1996, he joined the Communications Research Laboratory (CRL), Ministry of Posts and Telecommunications, Tokyo, Japan. He is currently a Research Manager at the National Institute of Information and Communications Technology (NICT), Tokyo. His current research interests include the area of photonic networks and optical communication technologies such as optical packet switching (OPS), optical processing, and optical code-division multiplexing (OCDM).

Dr. Wada received the 1999 Young Engineer Award from the Institute of Electronic and Communication Engineers, Japan, and the 2005 Young Researcher Award from the Ministry of Education, Culture, Sports, Science, and Technology. He is a member of the IEEE Communications Society (Comsoc), the IEEE Lasers and Electro-Optics Society (LEOS), the Institute of Electronics and Communications (IEICE), the Japan Society of Applied Physics (JSAP), and the Optical Society of Japan (OSJ).

Gabriella Cincotti (A'01–M'03–SM'06) was born in Naples, Italy, in 1966. She received the Laurea (M.Sc.) degree (cum laude) in electronic engineering from "La Sapienza" University of Rome, Rome, Italy, in April 1992.

From 1992 to 1994, she was a Project Engineer at the Microwave Laboratory, Alenia, Aeritalia and Selenia S.p.A., Rome. In October 1994, she was an Assistant Professor in the Department of Electronic Engineering, University of Roma Tre, Rome, where she became an Associate Professor in the Department of Applied Electronics in May 2005. She is the author or coauthor of more than 70 papers and presentations published in international journals and conferences.

Ms. Cincotti is a member of the IEEE Lasers and Electro-Optics Society (LEOS), the National Inter-University Consortium for Telecommunications (CNIT), and the Inter-University Research Centre for the Physical Agents Pollution (CIRIAF).

Ken-ichi Kitayama (S'75–M'76–SM'89–F'03) received the B.E., M.E., and Dr.Eng. degrees from Osaka University, Osaka, Japan, in 1974, 1976, and 1981, respectively, all in communication engineering.

In 1976, he joined the NTT Electrical Communication Laboratory. From 1982 to 1983, he was a Research Fellow at the University of California, Berkeley. In 1995, he joined the Communications Research Laboratory [currently, the National Institute of Information and Communications Technology (NICT)], Tokyo, Japan. Since 1999, he has been a Professor in the Department of Electrical, Electronic and Information Engineering, Graduate School of Engineering, Osaka University. He is the author or coauthor of more than 200 papers published in refereed journals and two book chapters, and has translated one book. He holds more than 30 patents. His current research interests include photonic networks and radio-on-fiber communications. He is currently an Associate Editor on the Editorial Boards of the IEEE PHOTONICS TECHNOLOGY LETTERS, the IEEE TRANSACTIONS ON COMMUNICATIONS, and the *Optical Switching and Networking*.

Dr. Kitayama is a Fellow of the Institute of Electronics, Information and Communication Engineers (IEICE), Japan. He received the 1980 Young Engineer Award from the IEICE, the 1985 Paper Award of Optics from the Japan Society of Applied Physics, and the 2004 Achievement Award of the IEICE.